MM Science Journal | www.mmscience.eu
ISSN 1803-1269 (Print) | ISSN 1805-0476 (On-line)
Special Issue | HSM 2019
15th International Conference on High Speed Machining
October 8-9, 2019, Prague, Czech Republic
DOI: 10.17973/MMSJ.2019_11_2019060

HSM2019-063

IN-PROCESS MONITORING AND ANALYSIS OF WHIRLING MOTIONS IN BORING AND TREPANNING ASSOCIATION DEEP DRILLING

A. Steininger[1]*, F. Bleicher[1]

[1]IFT – Institute of Production Engineering and Photonic Technologies, TU Wien, Vienna, Austria

*Corresponding author; e-mail: steininger@ift.at

Abstract
This work presents a holistic approach for monitoring machining processes of an industrial deep drilling machine. For that purpose, a machine tool was equipped with a multi-sensory monitoring system with the objective to detect and assess dynamic disturbances during the machining process. Disturbances are key characteristics of deep drilling processes and are intensified due to the high length-to-diameter-ratios. Consequently, the machining processes are sensitive to dynamic instabilities such as chatter and whirling vibrations. The developed monitoring application is highly versatile and enables conducting experimental investigations on boring and trepanning association (BTA) deep drilling, counter boring and skiving processes. Different signal processing techniques were implemented in the application, e.g. a continuous short-time Fourier transformation (STFT) for the determination of chatter and whirling vibration frequencies during the cutting process. With a non-proprietary machine-to-machine communication protocol, it is possible to regulate and control the machining processes based on the information gained during measurement and data analyses. Hence, it is possible to respond to process instabilities with a computerised procedure that is controlled by an algorithm.
Keywords:
BTA/ STS deep drilling; monitoring machining process; short-time Fourier transformation STFT; dynamic disturbances

1 INTRODUCTION

Taking up approximately 36% of primary processing time of all machining operations, drilling is one of the most important processes (considering a representative spectrum of work pieces) [Astakhov 2014]. One of the most common deep-drilling processes in solid drilling is Boring and Trepanning Association (BTA) drilling, which is also referred to as single-tube-system (STS) drilling. BTA drilling is employed for boring (counterboring) and core drilling (trepanning) applications. The STS/BTA is a type of deep hole drilling based on two special features: Firstly, the drill head has a special self-guided drill head [Sakuma 1981] with cemented carbide cutting inserts with an asymmetric arrangement that also leads to asymmetric process forces. Here, guide pads are used to support and guide the tool head in the bore hole being drilled. This self-guided application leads to a sliding movement of the pads along the lateral surface of the wall with additional levelling and smoothing effects on the surface microstructure [Abrahams 2017].

To protect the guide pads, it comes to the second feature of this technique. Compared to conventional drilling, the STS/BTA principle is supplying cooling lubricant under pressure. This lubricant is transported through an annular space between the bore wall and the boring bar to remove chips through narrowed chip passages on the tool head and the boring bar. As a result, the chips do not scratch the finished bore hole surface like in conventional drilling processes. Furthermore, the coolant lubricates the cutting zone and tends to reduce friction between the guide pads and the workpiece. A high volume flow of the cooling lubricant is responsible for flushing the chips via the chip mouth and the boring bar. This special forming or burnishing process decreases the surface roughness and leads to higher surface quality.

The STS/BTA method is applicable for diameters in a range from roughly 6 mm up to 1500 mm. Since-length-to-diameter ratios of up to 150 for slender tool-boring-bar assemblies are common [VDI 2006], the deep drilling process is sensitive to dynamic disturbances such as chatter and whirling vibrations. The present work presents an approach tackling the challenge of implementing a monitoring system for a STS process. With this flexible sensor integration, it is possible to monitor all kinematic operation modes of cutting and feed movements in deep drilling.

With the aim to predict the cutting forces and torque, the mechanics of conventional drilling have been investigated by Galloway [Galloway 1957]. Griffiths et al. [Griffiths 1993a] [Griffiths 1993b] developed a time invariant mathematical model to determine the cutting force system, the tangential pad forces and the friction coefficients for a

single cutting edge and two pads tool head configuration. Such modelled systems depend on functions of the chip thickness, width of cut, material properties, the cutting insert vibration at the current time *(t)* and one tooth period earlier *(t-τ)* [Altintas 2004]. However, when describing deep drilling processes mathematically additional parameters come into play: the tool head geometry [Matsuzaki 2015], the drilling depth (which leads to a shift in the natural frequency of the boring bar-tool head assembly [Weinert 2005]), the stiffness and guidance of the stuffing box [Gessesse 1991a], as well as of the Lanchester dampers and the own weight of the boring bar. Several studies investigated the dynamic behaviour of deep drilling for STS/BTA and gun drilling applications. Thai [Thai 1983], Chin [Chin 1996] and Weber [Weber 1978] developed analysis and time invariant models. Furthermore, detail investigations towards the dynamic behaviour of the bar in STS/BTA drilling were carried out by Chin et al. [Chin 1996] [Chin 1995] and Perng [Perng 1999].

The main dynamic disturbances during the STS/BTA deep hole machining are chatter vibrations and whirling/spiralling (helical multi-lobe formations). Whirling/spiralling describe process instabilities during drilling with polygonal shape effects towards the borehole. These holes can run into critical shape tolerances like roundness and cylindricity and have an impact on the produced component quality. Incidentally, the diameter may be within the tolerance if it is measured between two direct opposite points, since the resulting polygonal shape is a curve of constant width, which can be seen in Fig. 1 (b).

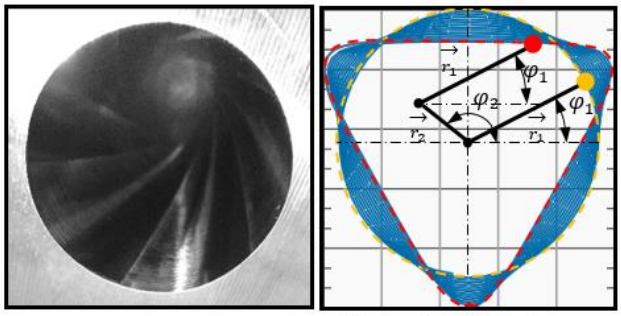

Fig. 1: (a) Spiralling of a polygonal shaped bore hole, (b) model to demonstrate the correlation of a rhodonea curve and a circle in polar coordinates.

Stockert [Stockert 1977] was one of the first authors, who investigated the effect of tool design parameters on whirling vibrations for STS/BTA drilling. He distinguished between three different origination points of whirling vibrations. The first is directly at the beginning of the process, the second is reproducible and occurs at the same drilling depth and third arises randomly. Gessesse et al. [Gessesse 1994] found a correlation between the whirling incidents and the second bending modes of the boring bar.

Whirling disturbances are able to arise when the frequency of the rotation or its higher orders coincide with the eigenfrequency of the bending mode of the boring bar. Consequently, whirling generates vibrations with frequencies of the rotational speed and its higher orders [Bayly 2002]. Studies on investigations on the eigenfrequencies of the boring bar have been published by Chin et al [Chin 1995] and Perng [Perng 1999]. Due to the constant varying drilling depth, it leads to shifts of the eigenfrequencies caused by the changing support situation. This subject has also been elaborated by Gessesse et al. [Gessesse 1991b] and Webber [Webber 2007]. Efforts in modelling the STS/BTA process and its vibration instabilities were made by Al Wedyan [Al-Wedyan 2007] Chin et al. [Chin 1996] Matsuzaki [Matsuzaki 2015] and Raabe [Raabe 2009]. Based on empirical data, they built models to predict critical process frequencies, where instabilities may occur.

2 MODELLING OF POLYGONAL SHAPED HOLES

Mathematically, a curve with a polygonal shape is a superposition of a circle and a rose or rhodonea curve. Such a curve is described by the formula (1) and is based on a sinusoid plotted in polar coordinates.

$$\begin{pmatrix} r_d \\ f_d \\ z_d \end{pmatrix} = \begin{pmatrix} r_1 + r_2 * \sin(x * f_{d1}) \\ f_{d1} \\ const. \end{pmatrix} \rightarrow f_d = (n_L * f_1) \quad (1)$$

The change from a circular motion, shown as yellow dashed line in Fig. 1 (b), to a polygonal motion, depicted as red dashed line in Fig. 1 (b), is caused by an amplitude modulation of the sinusoid part of the term r_d in formula (1). In Fig. 2 the term r_d is depicted as a curve over time where the amplitude modulation is represented by a linear growth function. By generating a three sided polygon (n_L=3) with an amplitude of 36 and a primary frequency of f_1=2 Hz, the resulting dominant frequency f_d is equal 6 Hz, see formula (1). This can be identified in the Fast-Fourier-Transformation (FFT) of the $r_d(t)$ signal in Fig. 2 (b).

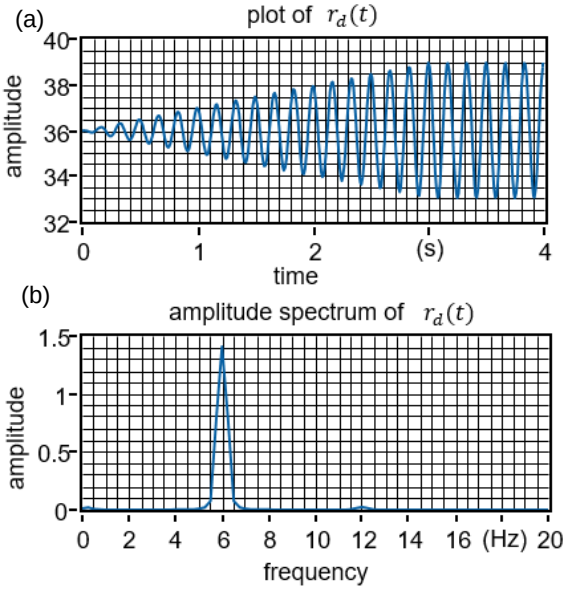

Fig. 2: Plot of $r_d(t)$, based on formula (1), over time with resulting amplitude spectrum

Curves with a polygonal shape can also be described by Cartesian equations and consist of two related circular motions, see formula (2). The physical principle is a double joint and is depicted in Fig. 1 (b).

$$\begin{pmatrix} x_d \\ y_d \\ z_d \end{pmatrix} = \begin{pmatrix} x_1 \\ y_1 \\ z_1 \end{pmatrix} + \begin{pmatrix} x_2 \\ y_2 \\ z_2 \end{pmatrix} \rightarrow$$

$$\begin{pmatrix} x_1 \\ y_1 \\ z_1 \end{pmatrix} = \begin{pmatrix} A_{x_1} * \sin\left(2\pi f_1 * t + \frac{2\pi * \varphi_{x_1}}{360}\right) \\ A_{y_1} * \cos\left(2\pi f_1 * t + \frac{2\pi * \varphi_{y_1}}{360}\right) \\ f_{rev} * t \end{pmatrix}$$

$$\begin{pmatrix} x_2 \\ y_2 \\ z_2 \end{pmatrix} = \begin{pmatrix} A_{x_2} * \sin\left(2\pi f_2 * t + \frac{2\pi * \varphi_{x_2}}{360}\right) \\ A_{y_2} * \cos\left(2\pi f_2 * t + \frac{2\pi * \varphi_2}{360}\right) \\ z_2 \end{pmatrix} \quad (2)$$

The superposition of two motions with the boundary conditions of a double joint results in a curve with a polygonal shape. The shape of the polygon curve can be modified by different kinematic conditions like the direction of rotation, the frequency and the radius. In Fig. 3 the Cartesian equations of two different polygon curves are shown as plots via time. The upper curves in Fig. 3 (a) are generated with a primary frequency f_1= *2 Hz* and a secondary frequency of f_2= *-4 Hz*. Despite the secondary frequency f_2= *8 Hz* the input parameters of the equations of the lower curves (Fig. 3b) are the same as of the upper curve. The polar plot of the upper and the lower $x_d(t)$ and $y_d(t)$ result both to a polygon curve with three lobes (n_L=*3).*

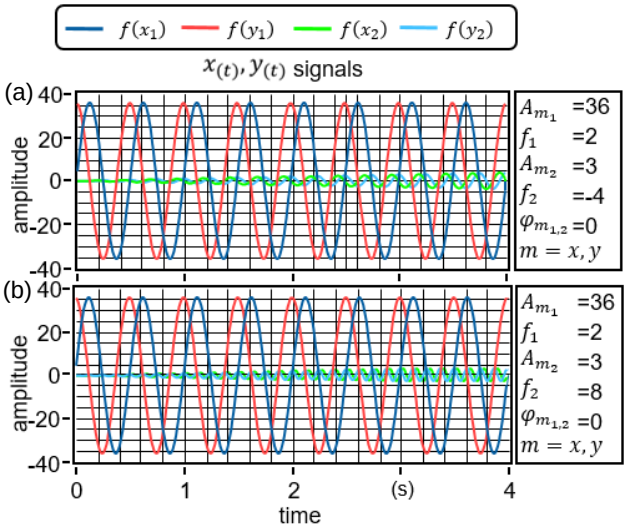

Fig. 3: Plot of $x_d(t)$ and $y_d(t)$, based on formula (2 and 3), over time with different secondary frequencies

Therefore, the secondary frequency f_2 is responsible for the number of generated lobes, thus it is the so called whirling frequency. The relationship of the primary and secondary frequency in the Cartesian equations, as well as the number of lobes is given in equation (4). Additionally, the relative direction of the whirling frequency towards the primary frequency affects the number of resulting lobes. If the primary and secondary frequency have the same rotational direction, the phenomena is called forward whirling. Accordingly, if the two frequencies show different rotational directions, it is called backward whirling.

$$f_2 = (n_L * f_1) \pm f_1 \quad (4)$$

Table 1 depicts the relation between the number of lobes and forward respectively backward whirling, exemplarily.

Table 1: Relation between numbers of lobes whirling frequencies

# of lobes	primary frequ. f_1	dominant frequ. f_d	whirling frequ. forward	whirling frequ. backward
(#)	(Hz)	(Hz)	(Hz)	(Hz)
3	2	6	8	4
4	2	8	10	6
5	2	10	12	8

The process of backward and forward whirling can be distinguished using a fast FFT of the time signal of the Cartesian function $x_d(t)$. As it is shown in Figure 4, a significant peak in the frequency domain can be seen for the primary frequency (2 Hz), whereas the secondary frequencies are also visible, though at 4 and 8 Hz, respectively. Under real-life conditions, forward and backward whirling via FFT are difficult to differentiate, since harmonic vibrations are usually superimposed.

As previously discussed in Fig. 3, two different input equations are used for the mathematical description of the phenomena. Fig. 5a shows the three dimensional polygon-curve of the input equations, describing forward whirling, whereas Fig. 5b shows the polygon curve for backward whirling. In Figure 5, the red curve indicates the outer radius of the cutting insert of a BTA drill head and the blue curve shows the outer radius of the inner cutting insert. In case of forward whirling, it can be seen that its shape resembles a flower petal, while for backward whirling a Reuleaux-triangle-shape can be observed. The red and the blue curve in Figure 5a and 5b are having a phase shift of 180°, as it can be also seen in the assembly of the drill head, depicted in Figure 6.

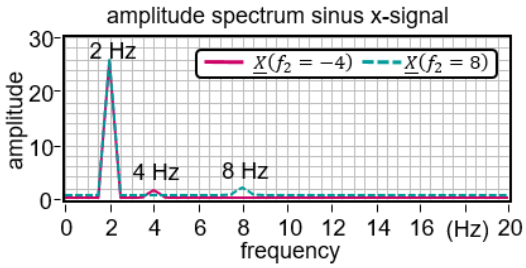

Fig. 4: Fast Fourier-Transformation graph of $x_d(t)$, backward whirling is depicted in red, whereas the dashed blue line depicts results of forward whirling.

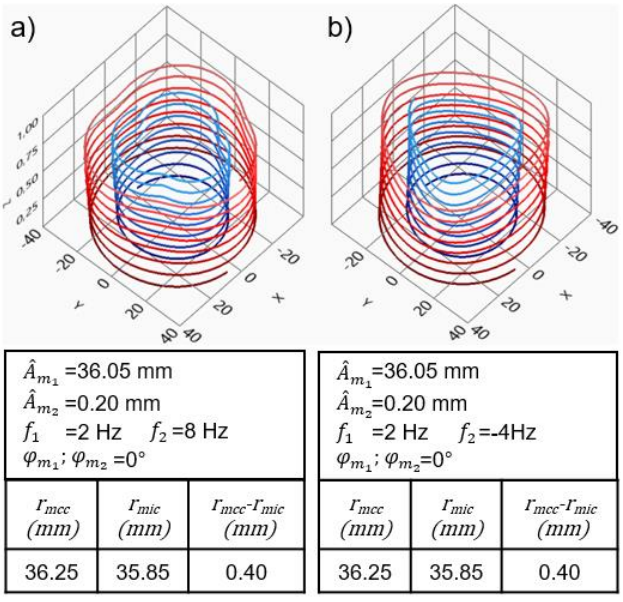

Fig. 5: Three-dimensional curve plot of the helical multi-lobe formations of the outer (red) and inner (blue) cutting radius caused by forward whirling (left) and backward whirling (right)

3 EXPERIMENTAL SETUP

To get deeper insights to the STS deep drilling process, a holistic process monitoring system was developed for the experimental investigations. A general overview is given in Fig.7a. Despite previous investigation [Steininger 2018], a new 12 m long tool-boring-bar assembly with length-to-diameter-ratios of up to 175 was developed and manufactured to investigate the process in deeper drilling depths.

As it is shown in Fig. 6, the STS drilling tool consisted of a tool head with an inner and an outer indexable carbide cutting insert. The three guide pads arranged at the outer diameter were exchangeable and were coated with a titanium nitride layer.

For measuring the dynamic process disturbances, sensory equipment was applied to the BTA machine tool. The measuring equipment was implemented towards the boring bar to determine the dynamic cutting forces. The sensor equipment was placed at the front end of the boring bar close to the STS tool head.

Due to the geometric shape of the boring bar; the force measurement devices were based on strain measurements reflecting the measurement of the thrust force, the bending moments/forces in the cutting force and the passive force direction. For providing comparability of the measured strain data, the current signal was calibrated with a multicomponent piezoelectric dynamometer (Kistler Type 9129AA).

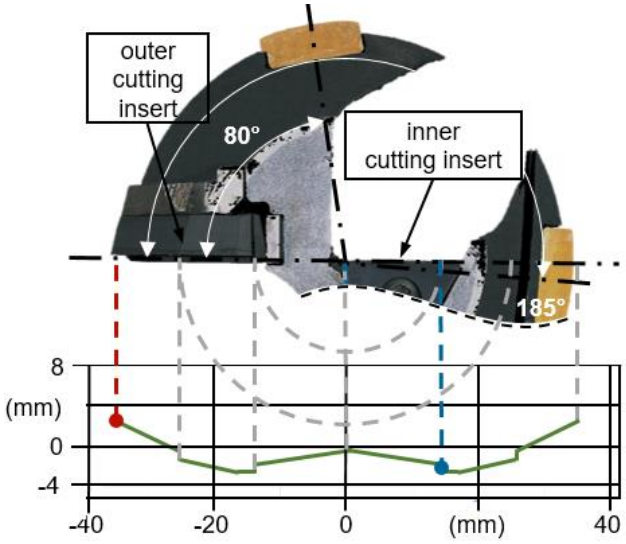

Fig. 6: Resulting cross-section of cut, limited by the outer (red line) and the inner cutting radius (blue) of the two inserts.

For measuring higher frequency characteristics of the dynamic process, vibration sensors and eddy current sensors were additionally installed at the boring bar. The stationary eddy sensors mounted at the oil pressure head, enabled the detection of process-induced dislocation of the boring bar.

For getting deeper insights in the process status, machine data was collected via a profibus gateway, which was installed at the Siemens control of the machine tool. It was possible to monitor several machine data like actual feed, rotational speed, z-position, drive power, override positions and the boring oil flow rate. In Fig. 7 (b) the principle of the machine communication is depicted. The basic machine-to-machine communication protocol was based on the non-proprietary OPC/UA communication protocol. By programming data blocks of the logic controller (PLC) it is possible to read and write machine data. In fact, this allows the user to influence the feed and spindle overrides of the machine tool in case of occurrence of unusual process parameters.

The OPC/UA standard gives the additional opportunity for transferring the machine data to further data processing systems like manufacturing execution system (MES). Tools like the presented approach enable planning machine and production utilization in a holistic and strategic manner.

Table 2 : Chemical composition of workpiece material in %

C	Mn	Cr	Mo	N	Ni
max. 0.06	20.50-21.60	18.30-20.00	min. 0.50	min. 0.60	min. 1.40

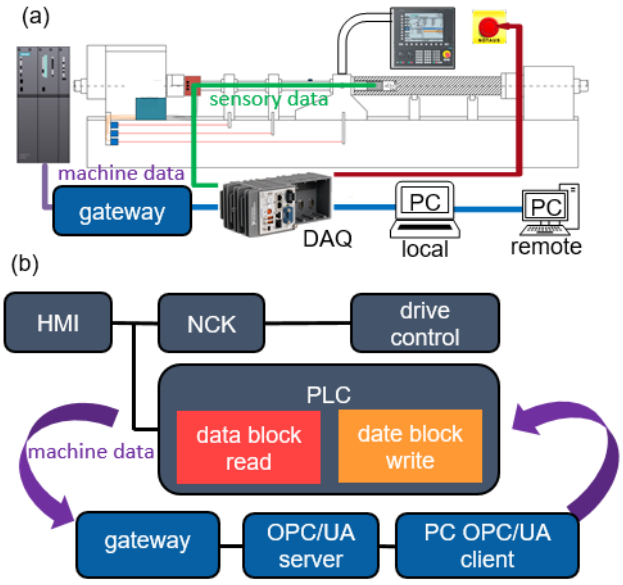

Fig. 7: (a) Overview of the machine monitoring setup at the boring machine, (b) overview of the machine data communication via profibus gateway and OPC/UA communication protocol

The workpiece material is a non-magnetic, austenitic Mn-Cr-steel with a high nitrogen content, see Table 2.

4 EXPERIMENTAL RESULTS

In the conducted machining tests, the focus was put on drilling with a steady tool-boring-bar assembly and a rotating workpiece. Diverse parameters were tested for analysing the chip formation related to the feed and the cutting speed.

As investigations from Thai [Thai 1983] and Gessesse et al. [Gessesse 1994] have shown, whirling is related to coincides of bending modes and multiples of the rotations frequency, and hence direct displacement measurements of the boring bar were conducted.

To intensify the likelihood of whirling vibrations, the drilled workpiece was not face turned. This lead to a poor axial run-out. During the tests, whirling originated at a drilling depth of 2.0 m and increased continuously up to a drilling depth of 2.5 m, where the process was stopped. The force measurements of this section are depicted in Fig. 8, where the continuous increase of the amplitude in the trust force and the cutting torque is visible. Due to the dynamic

disturbances, the signal quality was influenced as well. This can be observed in the normal distribution of a discrete signal period of one second. During normal cutting conditions, the force signals were typically normal distributed.

In addition, spectral measurements are performed by the monitoring software, as depicted in Fig. 9. In the online short-time Fourier transformation (STFT) the intensity of the spectral density rises for the lower frequencies. An FFT analysis of the discrete torque signal with the period of one second (at 400 seconds recording time) showed dominant frequencies at 6.7 Hz and 13.4 Hz. According to formula (1) and the parameters of the rotational frequency (2.23 Hz), it can be calculated that the resulting bore hole corresponds to a helical three-lobe formation. Also in the eddy-current signals, the same dominant frequencies were present.

process	material	machine	tool	workpiece number
STS drilling	Austenitic Mn-Cr-steel	deep hole drilling machine	Botek	GXXX6
diameter	**cutting speed**	**feed_Z1**	**rotational speed_SP1**	**rotational speed_SP2**
(mm)	(m/min)	(mm/min)	(U/min)	(U/min)
72.00	30	-20.39	0.00	134.12

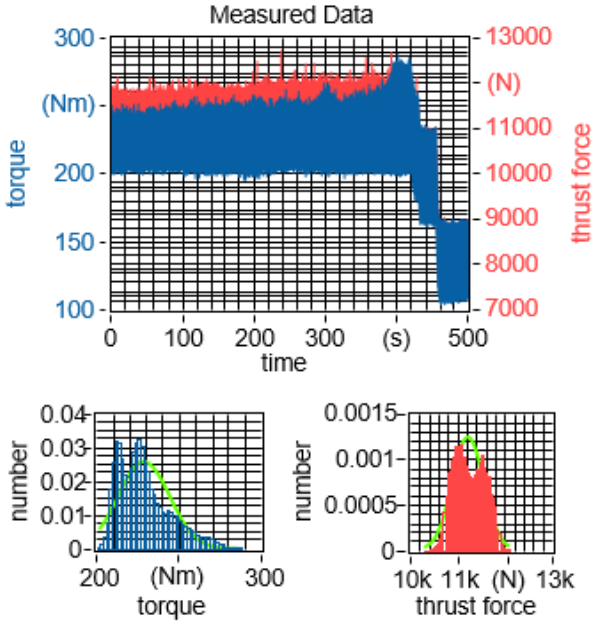

Fig. 8: Measurement of cutting forces during STS process

By generating a three dimensional polar plot of the two eddy-sensor signals in *X* and *Y-direction* and the feed in *Z-direction*, it was possible to detect the whirling direction of the tool centre point, see Fig.10 (b). Since the direction of the whirling motion is clockwise, whereas the workpiece is rotating counter clockwise during this machining test, it is possible to determine a so called back-whirling motion.

After the machining tests, the generated bore hole in the workpiece was investigated. For that purpose, the workpiece was cut in smaller specimens to conduct tactile roundness measurements. In Fig. 11, the roundness measurements of the polygonal shaped bore hole is depicted. It can be seen that the minimum circumscribed circle is d_{mcc} = 72,503 mm and the maximum inscribed circle is d_{mic} = 71,699 mm wide. The measured and calculated, Gauß-fitted mean diameter is d_m = 72,10 mm wide. Based on these measurements it is possible to calculate the input parameters for the mathematical model of formula (2). Consequently, Fig.5 shows the mathematical model of the polygonal curve, where the resulting maximum inscribed and minimum circumscribed circle fits exactly to the measurements, proving the applicability of the model.

The surface of the bore was investigated also under a microscope. In Fig. 11, the photographs of the bore surface show three material build ups via the circumference of the bore hole.

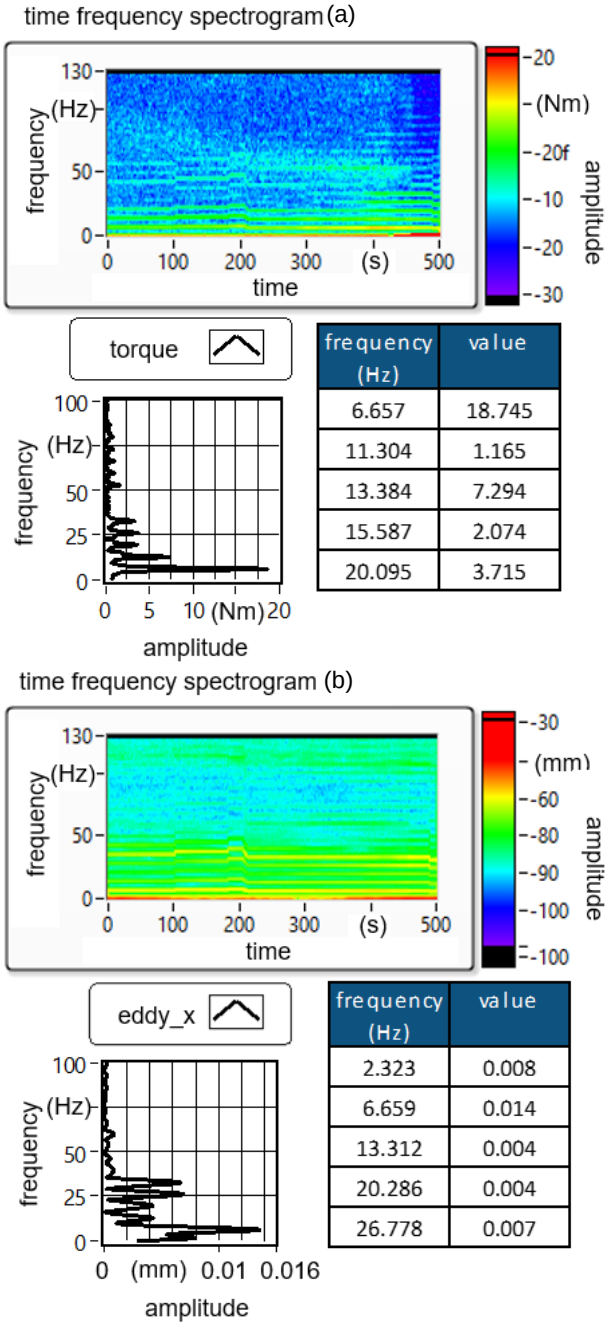

frequency (Hz)	value
6.657	18.745
11.304	1.165
13.384	7.294
15.587	2.074
20.095	3.715

frequency (Hz)	value
2.323	0.008
6.659	0.014
13.312	0.004
20.286	0.004
26.778	0.007

Fig. 9: Spectral measurements of the cutting torque during STS process

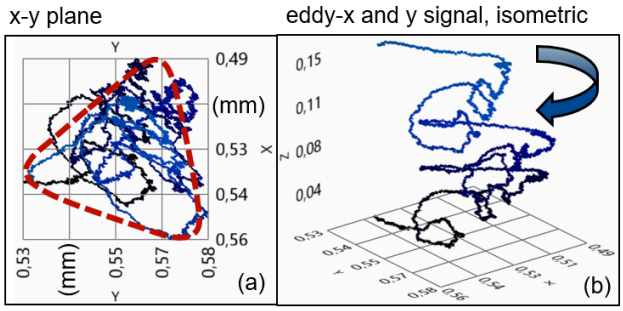

Fig. 10: Two- and three-dimensional polar plot of the two eddy sensor signals in x- and y- direction

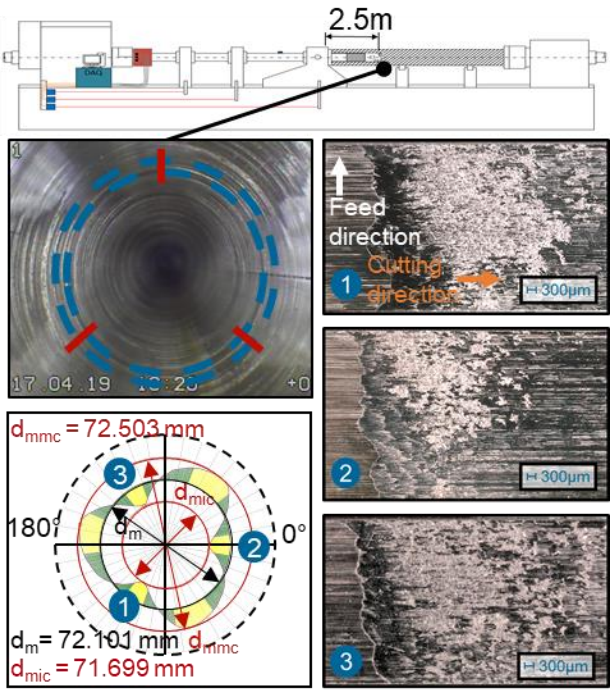

Fig. 11: Measurement directions of the monitoring system

5 CONCLUSION AND OUTLOOK

A refined monitoring approach for detecting dynamic disturbances for STS deep hole drilling was successfully developed within this study. Based on a previous monitoring system [Steininger 2018], a novel multisensory tool-boring-bar assembly with the length of 12 m was developed and tested. The flexible system with sensor integration provides the possibility of quick tool changes, making the system highly versatile and enabling different types of processes like STS deep drilling, counter boring and skiving. This system allows to detect dynamic disturbances during the process such as whirling or spiraling. A non-proprietary machine-to-machine communication was integrated to regulate the overrides of the machine based on the information gained by the sensor signals; the actual computerized procedure is based on threshold analysis. Further investigation aim at refinement of this algorithm to improve the detectability of dynamic disturbances.

Besides, a basic kinematic model was generated to understand the principle of the formation mechanism of helical multi-lobe formations. Based on sensor signals during the machining process and measurements of the resulted bore hole geometry, the model was successfully verified.

Future experiments will aim at drilling depth dependent chatter disturbances and other processes like counter boring and skiving.

6 REFERENCES

[Astakhov 2014] Astakhov, V. Drills: Science and Technology of Advanced Operations. ISBN 978-1-4665-8435-8, CRC Press, 2014

[VDI 2006] Verein Deutscher Ingenieure e.V. VDI 3210 Part 1 Deep-hole drilling. Berlin: Beuth Verlag, 2006

[Sakuma 1981] Sakuma, K. et al. Self-guiding action of deep-hole-drilling tools. Annals of the CIRP Vol.30 No.1,1981 pp. 311-315. doi.org/10.1016/S0007-8506(07)60948-2

[Abrahams 2017] Abrahams, H. Untersuchungen zum Führungsleistenverschleiß und zur Prozessdynamik beim BTA-Tiefbohren austenitischer Stähle. 2017.

[Galloway 1957] Galloway, D. F. Some experiments on the influence of various factors on drill performance. Transactions ASME, 1957.

[Griffiths 1993a] Griffiths, B. J. Modelling Complex Force Systems, Part 1 : The Cutting and Pad Forces in Deep Drilling. Journal of Engineering for Industry, May 1993, Vol. 115, pp. 169-176.

[Griffiths 1993b] Griffiths, B. J. and Grieve, R. J. Modelling Complex Force Systems, Part 2: A Decomposition of the Pad Forces in Deep Drilling. Journal of Engineering for Industry, May 1993, Vol. 115, pp. 177-183.

[Altintas 2004] Altintas, Y. and Weck, M. Chatter Stability of Metal Cutting and Grinding. Annals of the CIRP,January 2004, Vol. 53, No. 2, pp.619-642. doi.org/10.1016/S0007-8506(07)60032-8

[Matsuzaki 2015] Matsuzaki, K. et al. Theoretical and experimental study on rifling mark generating phenomena in BTA deep hole drilling process (generating mechanism and countermeasure). International Journal of Machine Tools & Manufacture, January 2015, Vol. 88, pp. 194-205. doi.org/10.1016/S0007-8506(07)60032-8

[Weinert 2005] Weinert, K. et al. On the influence of drilling depth dependent modal damping on chatter vibration in BTA deep hole drilling. , CIRP Ann.-Manuf. Technol., 2005, Vol. 54, No. 1, pp. 363-366. doi.org/10.1016/S0007-8506(07)60123-1

[Gessesse 1991a] Gessesse, Y. B. and Latinovic V. N. Effect of the stiffness characteristics of the stuffing box on boring bar vibrations. Int. J. Prod. Res., March 1991, Vol. 29, No.3, pp. 565-574. doiorg/10.1080/ 00207549 108930089

[Thai 1983] Thai, T.P. Beitrag zur Untersuchung der selbsterregten Schwingungen von Tiefbohrwerkzeugen. 1983.

[Chin 1996] Chin, J. H. and Lin S. A. Dynamic Modelling And Analysis Of Deep-Hole Drilling Process. Int. J. Model. Simul. January 1996, Vol. 16, No. 3, pp. 157-165. doi.org/10.1080/02286203.1996.11760295

[Weber 1978] Weber U. Beitrag zur messtechnischen Erfassung des Tiefbohrprozesses, 1978.

[Chin 1995] Chin, J.H. and Lee, L. W. A study on the tool eigenproperties of a BTA deep hole drill—theory and experiments. Int. J. Mach. Tools Manuf., January 1995, Vol. 35, No. 1, pp. 29-49. doi.org/10.1016/0890-6955(95)80007-7

[Perng 1999] Perng, Y.L. and Chin, J. H. Theoretical and experimental investigations on the spinning BTA deep-hole drill shafts containing fluids and subject to axial force. Int. J. Mech. Sci., November 1999. Vol. 41, No. 11, pp. 1301–1322. doi.org/10.1016/S0020-7403(98)00091-5

[Stockert 1977] Stockert R. Dralleffekte beim Tiefbohren VDI Berichte, 1977,(301), pp.73-80.

[Gessesse 1994] Gessesse, Y. B. et al. On the Problem of Spiralling in BTA Deep-Hole Machining. J. Eng. Ind., May 1994, Vol. 116, No. 2, p. 161. doi:10.1115/1.2901926

[Bayly 2002] Bayly, P.V. et al. Low-Frequency Regenerative Vibration and the Formation of Lobed Holes in Drilling. J. Manuf. Sci. Eng., 2002, Vol. 124, No. 2, p. 275. doi:10.1115/1.1459087

[Gessesse 1991b] Gessesse, Y. B. and Latinovic V. N. Effect of the stiffness characteristics of the stuffing box on boring bar vibrations. Int. J. Prod. Res., March 1991, Vol. 29, No. 3, pp. 565–574.

[Webber 2007] Untersuchungen zur bohrtiefenabhängigen Prozessdynamik beim BTA-Tiefbohren. Vulkan-Verlag GmbH, 2007.

[Al-Wedyan 2007] Al-Wedyan, H.M. et. al. Whirling Vibrations in Boring Trepanning Association Deep Hole Boring Process: Analytical and Experimental Investigations. J. Manuf. Sci. Eng., 2007, Vol. 129, No. 1, p. 48.

[Raabe 2009] Raabe, N. et al. Dynamic Disturbances in BTA Deep-Hole Drilling: Modelling Chatter and Spiralling as Regenerative Effects. Advances in Data Analysis, Data Handling and Business Intelligence. Springer Berlin Heidelberg, July 2009, pp. 745–754. DOI 10.1007/978-3-642-01044-668

[Steininger 2018] Steininger, A. and Bleicher, F. In-process monitoring and analysis of dynamic disturbances in boring and trepanning association (Bta) deep drilling. J. Mach. Eng., November 2018, Vol. 18, pp. 47–59. doi.org/10.5604/01.3001.0012.7632